Papers

Sea level and storm surge forecasting in the Southern Baltic*

OCEANOLOGIA, No. 31
pp. 5–23, 1991.
PL ISSN 0078–3234

Sea level
Sea forecasting
Baltic Sea
Storm surge

ANDRZEJ WRÓBLEWSKI
Institute of Oceanology,
Polish Academy of Sciences,
Sopot
81-967 al. Powstańców Warszawy 55

Manuscript received March 13, 1991, in final form November 18, 1991.

Abstract

The paper presents an application of the multiple regression of dynamic systems and empirical orthogonal functions to sea level forecasting at five Polish ports on the Baltic coast with a lead time of 24 h. An assumption of the sea level changes approximated by superimposing of long- and short-period oscillations has been employed. The sea level and atmospheric pressure data were attributed to these oscillations by the use of a recursive low-pass filter. The hindcast characteristics obtained, as well as the computations based on independent measurement data, indicate the effective operation of the model during everyday sea level changes and storm surges.

1. Introduction

Empirical orthogonal functions (EOF) were employed in sea level forecasting for the first time by Holmström and Stokes (1978) and Törnevik (1977). These forecast models have been in constant use since 1979. Similar models worked out for the Swedish coasts in the region of the Danish Straits, used since 1981, were presented by Nyberg (1983). The employment of these forecasts involves sampling the sea level and atmospheric pressure at 12 h intervals. EOF have also been used for analyzing the sea level variability, and for relating this phenomenon to the variability of the atmospheric

* The investigations were carried out as part of the research programme CPBP 03.10, co-ordinated by the Institute of Oceanology of the Polish Academy of Sciences.

pressure and wind fields (Nielsen, 1979; Thompson, 1979). The possibilities of applying EOF to the computation of storm surges for short lead times have been discussed in a separate paper (Wróblewski, 1986). The application of these functions in investigations of dynamic processes in the open sea and coastal zone is also known.

The solutions presented in the following constitute an attempt at formulating effective forecast models for the nontidal sea waters of the Polish coastal area. In order to obtain reliable results of sea level changes during stormy periods, it has been assumed that the process under discussion is a superimposition of separately determined oscillation components. The interval forecast has also been introduced. The general forecast method was elaborated earlier (Wróblewski, 1990). In this work the storm surge computations are presented in detail.

2. Measurement data

The models were identified and the parameters estimated on the basis of the measurement period from 1 January 1978 to 31 December 1979. Sea levels were recorded by means of tide gauges at Świnoujście, Kołobrzeg, Ustka, Władysławowo and Gdynia. Atmospheric pressures at sea level were taken from synoptic charts at the twelve grid nodes shown in Figure 1.

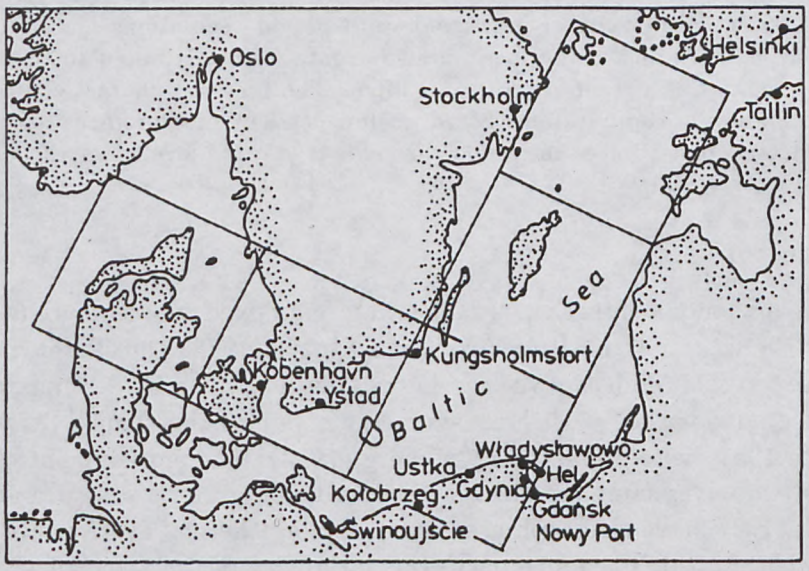

Fig. 1. Geographical position of the analyzed tide gauge stations and of the atmospheric pressure grid

Data with a sampling interval of $\Delta t = 3$ h were taken into account in the computations. The models were verified using independent observations for the periods 1 January 1968 – 30 May 1968 and 1 October 1968 – 31 October 1968, selected because of the considerable dynamism of the sea level changes. The seven greatest storm surges from the period 1970–1983 are also included. The data were obtained from the Institute of Meteorology and Water Management (1983).

3. Assumptions of the forecast model

As already indicated, a data sampling interval of 3 h is assumed. In view of the dynamism of Baltic water level changes, very good results can be obtained by employing longer sampling intervals, since the majority of oscillations are slow enough for everyday changes to be recorded at intervals of > 10 h with an accuracy sufficient for practical purposes. When estimating the parameters of the forecast model for long data series, the results are therefore influenced by both the sampling interval and the average dynamic conditions during the measurement. Under such conditions the model applies very well for changes of sea level forced by wind and atmospheric pressure fields characterized by periodicity close to that of middle and long periods recorded during the investigations. However, it should be emphasized that the above statement does not apply to non-typical situations occuring during sudden gusts of wind against the sea surface. Such wind conditions are related to the rapid displacement of lows over the Baltic. Though constituting less than 1% of the general variance of the phenomenon, the extremely high resultant sea levels present a hazard to shipping and shore defences.

In this situation, formulating a linear dynamic statistical model of the linear relations between the everyday changes in this phenomenon and the nonlinear rapid rising and falling of the sea level is a complex problem. The practical difficulties also result from the fact that atmospheric pressure field forecasts are supplied at intervals exceeding $\Delta t = 3$ h. This data sampling interval was, however, taken into account when this problem was investigated. In the case of violent and strong winds, the introduction of interpolated atmospheric pressure data into the computations seemed to be the only solution to the problem. The time lag in the response of the water surface to gale force winds ranges from 4 to 6 h for the Baltic. Hence, it is obvious that during rapid sea level changes, forecasts should be issued every three hours. Moreover, in order to take nonlinear effects into account, sea level changes were assumed to be superimpositions of long- and short-period oscillations. Such oscillations of the sea level and atmospheric pressure were separated by the use of a first-order low-pass recursive filter, the characteristics of which

were sufficient for this application. Filtration carried out with a coefficient $\gamma = 0.7$ enabled the long-period variability to be taken into account by the use of data close to the daily mean values, as is demonstrated by the filtration characteristics shown for real time in Figure 2. The filter transmittance is given by the formula (Otnes and Enochson, 1972)

$$H(f) = \frac{1-\gamma}{1-\gamma\exp(-j2\pi\Delta t f)}. \tag{1}$$

The squared absolute value of the transfer function is given by

$$H(f)^2 = \frac{(1-\gamma)^2}{1-2\gamma\cos 2\pi f\Delta t+\gamma^2}. \tag{2}$$

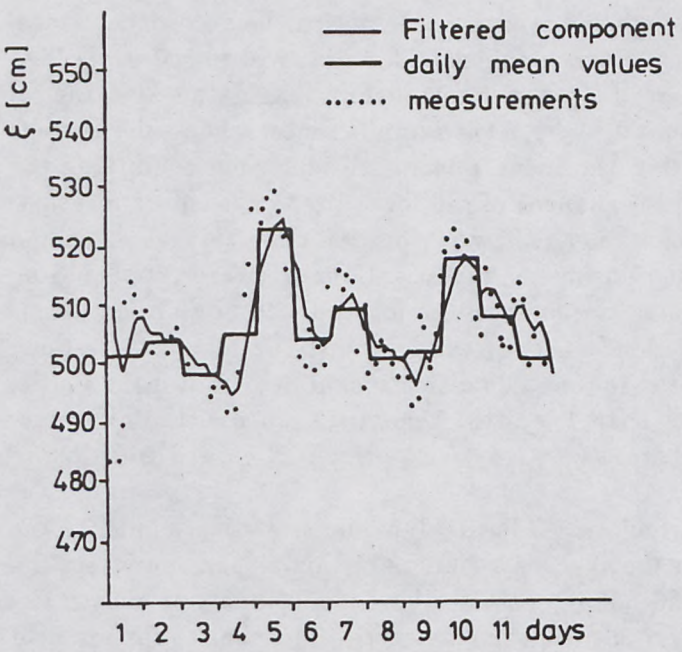

Fig. 2. Low-pass filtration of sea levels

When describing the differentiation of the oscillations into long- and short-period ones, the conventionality of the nomenclature should be pointed out, since the filter employed did not separate the periodical components distinctly. As the computations of the sea level coherence between the tide gauges in Gdańsk and Świnoujście have shown, all sea level changes with periods of 40 h and longer are common on the Polish coast. When analyzing periods shorter than 40 h, it has been found that, for all the stations considered, coherence indicates the occurrence of tides with amplitudes up to 1 cm, and of rare overall Baltic seiches resulting in level changes of the order of up

to 10 cm (Kowalik and Wróblewski, 1973). Under such conditions, the employment of another type of filtration with sharp characteristics, separating oscillations with periods from 6 h to, say, 24 h, would lead to uncorrelated data being obtained at particular tide gauge stations, thus precluding the employment of EOF in forecasting there.

4. Forecast model

At the beginning of the model construction, the matrices of long- and short-period oscillations of sea levels and atmospheric pressures were expanded according to the EOF scheme. For sea levels this expansion is given by

$$\mathbf{Z} = \boldsymbol{\beta}\mathbf{H}, \tag{3}$$

where

$\mathbf{Z}$ – matrix of the sea level oscillation components with elements $z_i(t)$, $i = 1, ..., M$; $t = 1, ..., N$,

$\mathbf{H}$ – square matrix of the normalized local transfer functions with elements h_{ni}, $n = 1, ..., M$; $i = 1, ..., M$,

$\boldsymbol{\beta}$ – matrix of the amplitude functions with elements $\beta_n(t)$, $n = 1, ..., M$; $t = 1, ..., N$,

$M = 5$ – number of measurement series,

$N = 5840$ – number of data in the measurement series.

Table 1. Convergence of the sea level and atmospheric pressure expansion in the EOF amplitude functions as an overall variance percentage of the variability of the phenomenon

n	1 [%]	2 [%]	3 [%]	4 [%]	5 [%]	Total percentage of five amplitude functions
Long-period oscillations						
$\mathrm{Var}\alpha_n(t)$	87.0	8.3	3.7	0.4	0.2	$\mathrm{Var}^5\alpha_n(t) = 99.6\%$
$\mathrm{Var}\beta_n(t)$	95.0	4.0	0.5	0.3	0.2	$\mathrm{Var}^5\beta_n(t) = 100\%$
Short-period oscillations						
$\mathrm{Var}\alpha_n(t)$	71.0	14.6	7.4	2.1	1.3	$\mathrm{Var}^5\alpha_n(t) = 96.4\%$
$\mathrm{Var}\beta_n(t)$	79.7.	12.9	4.3	2.1	1.0	$\mathrm{Var}^5\beta_n(t) = 100\%$

The physical sense of the normalized local transfer functions lies in the presentation of mutually orthogonal sea level systems along the coast. The plots of these functions are shown in Figure 3. The convergence of the amplitude functions as related to the overall sea level variance obtained from measurements is shown in Table 1. Detailed analysis of the course of the

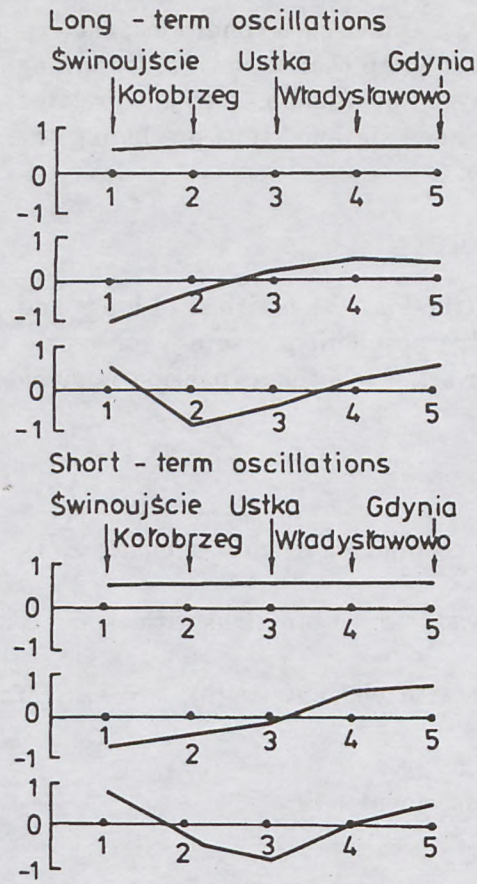

Fig. 3. Local transfer functions of sea levels for long and short-period oscillations

amplitude functions indicates that the first function related to simultaneous rises or falls in sea level at all measuring stations covers the highest percentage of the overall variance, and also represents the long-period oscillations of the phenomenon. The remaining amplitude functions represent the successive sea level configurations shown in Figure 3, whose decreasing overall variance percentage are related to the oscillations with decreasing periods. The time dependent amplitude functions in the expansion represent the effect of time-independent local transfer functions on the sea level. An important problem in further computations was to select amplitude functions with a physical sense which did not represent the noises of the variance-covariance matrix. This could be accomplished by employing the method of Preisendorfer and Barnett (1977). In this solution, not only the determination of the amplitude functions having a physical sense, but also the assumption of functions which could be computed within the framework of the model were of importance. Thus, the number of the amplitude

functions was reduced by using as a criterion the possibility of determining them using the model presented later. Since the model is justified by the dynamic character of the relationship between the sea level and the pressure field interaction over the Baltic, it is obvious that the functions thus selected have a real physical meaning. On the basis of these assumptions, three first – amplitude functions were used in further computations, together covering 99.5% of the variance of the long-period oscillations, and 96.9% of the short-period oscillations.

The expansion of the atmospheric pressure field in EOF amplitudes was in principle carried out in a way similar to that of the sea levels, by separating the first two oscillation components. It is then given by

$$\mathbf{G} = \boldsymbol{\alpha}\mathbf{D}, \tag{4}$$

where

$\mathbf{G}$ – matrix of the atmospheric pressure oscillation components with elements $g_i(t)$; $i = 1, ..., M$; $t = 1, ..., N$,

$\mathbf{D}$ – square matrix of normalized local transfer functions with elements d_{ni}; $n = 1, ..., M$; $i = 1, ..., M$,

$\boldsymbol{\alpha}$ – matrix of the amplitude functions of the expansion with elements $\alpha_n(t)$; $n = 1, ... M$; $t = 1, ..., N$,

$M = 12$,

$N = 5840$.

Physical interpretation of the matrix $\mathbf{D}$ consists of determining the individual schemes of isolines on a plane defined by the assumed grid, and of analizing the system thus determined in the form of orthogonal components of the atmospheric pressure field. In this approach, the individual series of matrix $\boldsymbol{\alpha}$ represent the effect of the time-independent orthogonal field components on the current atmospheric situation as a function of time. The convergence of this expansion is shown in Table 1. The considerable convergence of the expansion for a small number of amplitude functions can be accounted for by the limited area and the number of offshore grid points and minimizes the number of coastal measurement stations. The amplitude functions selected for the model were truncated by accepting those functions for further computations which improved computation effectiveness. Thus, the four first functions $\alpha_n(t)$ were determined, representing 99.4% of the variance of long- and 95.1% of that of short-period oscillations. It should be emphasized that the amplitude functions of the expansion represent both the atmospheric pressure and the wind fields, which results from the representation of the atmospheric pressure field components by local transfer functions. As is well-known, every atmospheric pressure system of isobars is related to the wind field. If a linear relationship is assumed between the horizontal component of the atmospheric pressure gradient for a

given point and the wind transformed by the local topography of the area, then the wind field covered by the grid is represented by the matrix $\vec{\mathbf{W}}$, the elements of which are $\vec{w}_j$ at point j. The elements are the vector sums of winds created by orthogonal configurations of the pressure field components

$$\vec{w}_j = \vec{w}_{1j} + \vec{w}_{2j}, \ldots + \vec{w}_{Mj}. \tag{5}$$

The systems of the first four local transfer functions of long-period oscillations are shown in Figures 4 and 5.

The expansion of the sea levels and the atmospheric pressure fields according to the EOF scheme is discussed briefly since this problem has been analyzed in detail in the literature referred to in the introduction to the present paper.

The construction of the forecast model has in principle been based on the assumption that the amplitude functions of the sea level are determined for the individual oscillations by the use of multiple regression equations for dynamic systems. This assumption can be given by

$$\mathbf{z} = \mathbf{X}\mathbf{p} + \mathbf{v}, \tag{6}$$

where

$$\mathbf{z} = [z_1, z_2, z_3, \ldots, z_N]^T, \tag{6a}$$

$$\mathbf{X} = \begin{bmatrix} \mathbf{x}_1 \\ \mathbf{x}_2 \\ . \\ . \\ . \\ \mathbf{x}_{N-1} \\ \mathbf{x}_N, \end{bmatrix} \tag{6b}$$

$$\mathbf{v} = [v_1, v_2, v_3, \ldots, v_N]^T, \tag{6c}$$

$$\mathbf{p} = [p_1', p_2', \ldots, p_m', p_o, p_1, p_2, \ldots, p_s]^T, \tag{6d}$$

$$\mathbf{x}_n = [-z_{n-1}, \ldots, -z_{n-m}, x_n, x_{n-1}, \ldots, x_{n-s}], \tag{6e}$$

$$v_n = e_n + a_1 e_{n-1}, \ldots, + a_r e_{n-r}, \tag{6f}$$

$$E(e_n) = 0; \qquad E(e_n^2) = \sigma^2, \tag{6g}$$

$\mathbf{z}$ – output series vector,
$\mathbf{X}$ – substitute input matrix,
$\mathbf{p}$ – parameter vector; p' are parameters for output series,
$\mathbf{v}$ – substitute correlated noise vector,
e_n – uncorrelated noise.

Vector $\mathbf{p}$ in formula (6) is estimated by the regression methods applied to dynamic systems. The sea levels are next computed as a superimposition of long- and short-period components, employing the basic relationships given by the matrix formula (3)

a

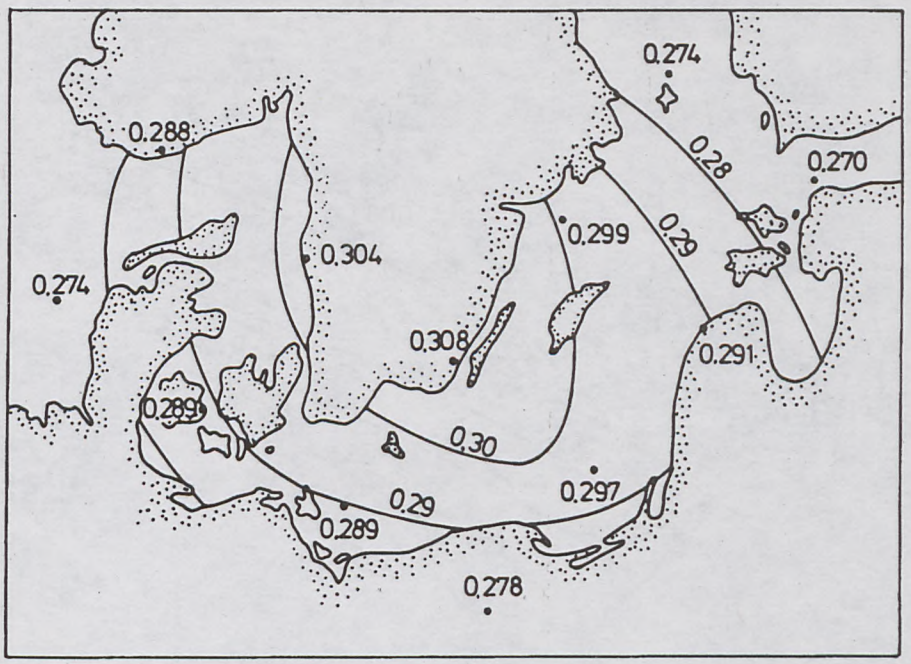

b

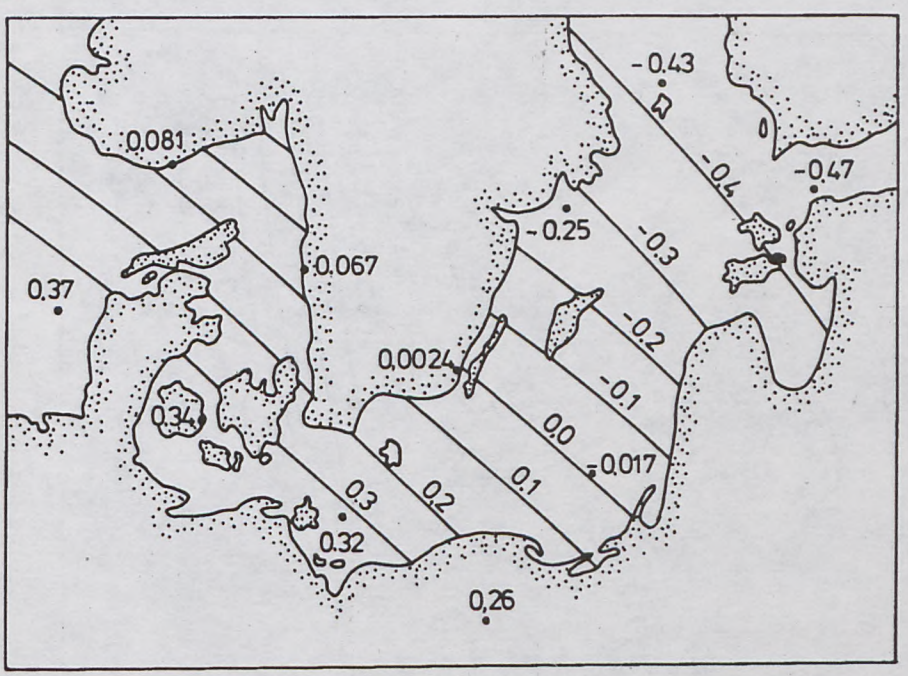

Fig. 4. Local transfer functions, d_{1i}(a) and d_{2i}(b), of long-period atmospheric pressure oscillations

a

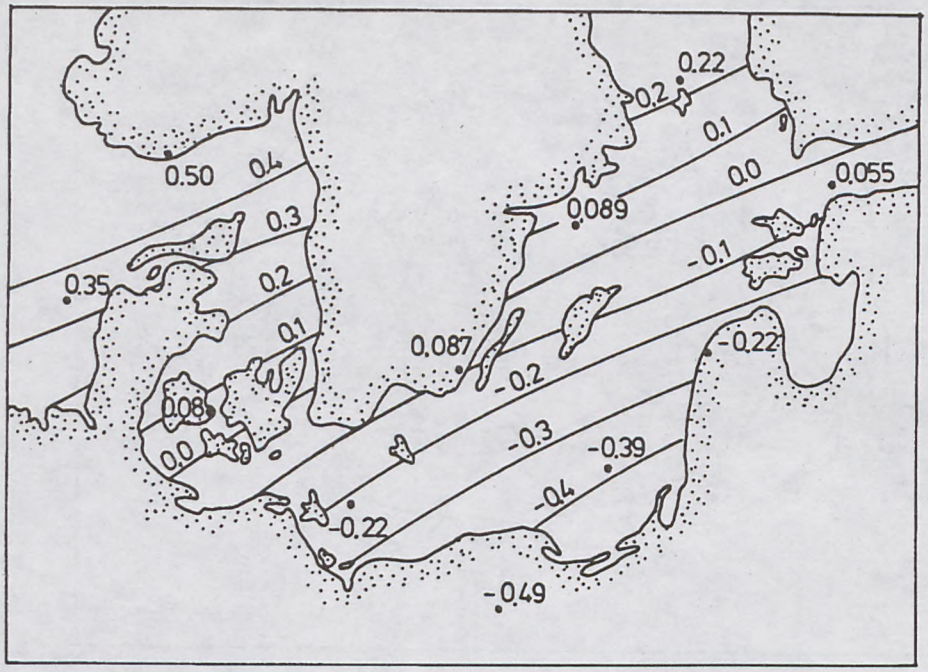

b

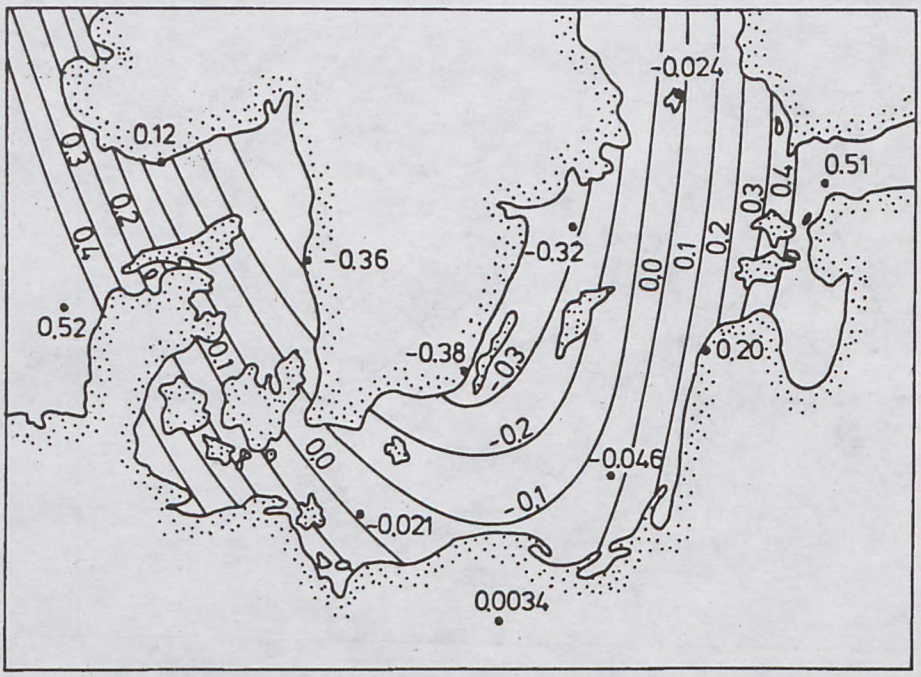

Fig. 5. Local transfer functions, d_{3i}(a) and d_{4i}(b), of long-period atmospheric pressure oscillations

$$\hat{\xi} = \mathbf{Z}_L + \mathbf{Z}_S, \tag{7}$$

$$\hat{\xi} = \beta_L \mathbf{H}_L + \beta_S \mathbf{H}_S, \tag{7a}$$

$$\mathbf{V} = \xi - \hat{\xi}, \tag{7b}$$

where

ξ – sea level matrix,

$\mathbf{V}$ – error matrix,

L, S – respective indices of long-period and short-period oscillations.

Having the above in mind, a brief presentation of the model can be confined to the determination of a general formula for the rows of the predictor matrix $\mathbf{X}'$, with the dynamic character of these relationships being taken into account. The respective formulae, chosen as a result of diagnostic computations, are given below for the lead time t which precedes the last measurements data by 24 h

- long-period oscillations:

$$\mathbf{x}'_t = [B^{48}\beta_n(t) + B^{24}\beta_n(t) + B^{48}\alpha_m(t) + B^{24}\alpha_m(t) + \alpha_m(t)], \tag{8}$$

- short-period oscillations:

$$\mathbf{x}'_t = [B^{9}\alpha_m(t) + B^{6}\alpha_m(t) + B^{4}\alpha_m(t) + B^{3}\alpha_m(t) + \alpha_m(t)], \tag{9}$$

where

B – back shift operator,

n – 1,..., 3,

m – 1,..., 4.

It is seen from formula (9) that the component of short-period oscillations is affected only by the variations in the atmospheric pressure field immediately preceding the forecasted sea level. The data should be obtained from the atmospheric pressure field forecast and interpolated with respect to the forecast lead time and assumed sampling interval. In the formula describing the long-period oscillations, the last term only refers to the atmospheric pressure field forecast. The remaining terms of the formula should be obtained from current measurements. Matrices $\mathbf{X}'$ do not, however, constitute the ultimate set of the prediction series. They also include the correlated data series, the number of which is too high. The number of the predictor series was lowered and orthogonalized by repeatedly expanding

Table 2. Prediction series for individual functions $\beta_n(t)$ according to the numeration of the amplitude functions in matrix $\mathbf{X}$

Amplitude function of the sea level	Numeration of matrix $\mathbf{X}$ series	
	Long-period oscillations	Short-period oscillations
$\beta_1(t)$	1, 2, 3, 5, 7, 8, 10, 14, 16	1, 3, 4, 5, 6, 8, 14
$\beta_2(t)$	1, 2, 3, 6, 7, 9, 12, 14, 16	1, 2, 3, 4, 5, 7, 8, 14
$\beta_3(t)$	1, 2, 3, 4, 5, 6, 8, 10, 15	1, 3, 4, 5, 7, 9, 14

matrix $\mathbf{X}'$ according to the EOF scheme. The amplitude series obtained were selected using the cross-validation method, thus creating the ultimate predictor matrix $\mathbf{X}$ (Golub and Heath, 1979; Lachenbruch and Goldstein, 1979). The results of the prediction series selection are summarized in Table 2.

5. Computations

Preliminary computations were carried out with the material obtained during a two-year period. The results are given in Table 3. The data given therein indicate that in spite of accepting solutions enabling rapid sea level

Table 3. Characteristics of hindcast computations of sea level changes along the Polish coast at intervals of $\Delta t = 3$ h for the period from 1 January 1978, to 31 December 1979

Tide gauge	σ_v [cm]	$< \lvert v \rvert >$ [cm]	$\bar{v}$ [cm]	$\mathbf{E}(\mathbf{X}^T\mathbf{v})$
Świnoujście	9.2	6.2	0	**0**
Kołobrzeg	9.0	6.1	0	**0**
Ustka	8.1	5.2	0	**0**
Władysławowo	7.7	4.8	0	**0**
Gdynia	6.9	4.5	0	**0**

Notation used in Table 3:

σ_v – r.m.s. error of the hindcast,

$< \lvert v \rvert >$ – mean of absolute values of the hindcast error,

$\bar{v}$ – mean value of the hindcast error,

$\mathbf{E}(\mathbf{X}^T\mathbf{v})$ – vector of correlation between predictor matrix and error vector; when the correlation is not meaningful at a significance level of 0.05, a zero value is assumed.

changes to be taken into account to a greater extent, the general hindcast characteristics for a two-year period are evidence for the satisfactory operation of the model. The increase in the r.m.s. error of the computations when passing from Gdynia to Świnoujście accords with the general characteristics of the Baltic water level changes along the longitudinal axis parallel to the coast. It can be shown for further characterization of the model that the r.m.s. error of a 24 h persistent forecast amounts to 10 cm for Gdynia, increasing gradually, when passing through the intermediate stations, to 13 cm for Świnoujście. The range of the sea level changes in the period of 1951–1970 amounted to 192 cm for Gdynia and 273 cm for Świnoujście. The results obtained can be compared with the respective Swedish data for tide gauge stations situated on the opposite shore of the sea (see Fig. 1). The

r.m.s. hindcast errors for Kungsholmsfort and Ystad have been computed as 6.1 and 8.5 cm respectively for a long data period[1]. The series of residues analyzed did not satisfy the assumptions of normal distribution. The empirical distributions obtained are summarized in Table 4. Verification by von

Table 4. Empirical probability of the occurrence of errors according to hindcast computations for the period 1 January 1978 – 31 December 1979

Interval	Empirical probability for occurrence in the interval					Probability according to N(0, 1)
	Świnoujście [%]	Kołobrzeg [%]	Ustka [%]	Władysławowo [%]	Gdynia [%]	[%]
$(-\sigma_v, \sigma_v)$	79.1	80.3	78.7	79.2	79.9	68.3
$(-2\sigma_v, 2\sigma_v)$	95.3	96.1	95.7	95.8	95.6	95.5
$(-3\sigma_v, , 3\sigma_v)$	98.4	98.6	98.6	98.8	98.9	99.7
$(-4\sigma_v, 4\sigma_v)$	99.3	99.3	99.3	99.7	99.8	100.0

Neuman's test did not confirm the hypothesis of the independence of the individual series of matrix **V** for forecasts computed every 3 h. It is worth mentioning that in everyday practice the forecast should be computed every 12 h. It can be assumed for this forecast interval that the hypothesis of the independence of the error series will not be rejected. A forecast interval of 3 h is only needed in the case of storm surges.

Better joint characteristics of the model for all the ports considered, computed for the data from Tables 3 and 4, are given in Table 5.

Table 5. Total forecast accuracy for five ports analyzed according to hindcast computations for the period 1 January 1978 – 31 December 1979

Smoothed empirical probability	Hindcast r.m.s. interval for five ports
79%	7 cm – 9 cm
96%	14 cm – 18 cm
99%	21 cm – 28 cm

The results presented so far refer to the measurement period for which the identification of the model and estimation of parameters were carried out. For ultimate verification of the model, computations for independent observational material are indispensable. To this end, the periods of 1 January 1968 – 30 May 1968, and 1 October 1968 – 30 October 1968, were chosen, characteristic of which are the considerable dynamics of the sea level

[1]Data taken from graphs by Holmström and Stokes (1978).

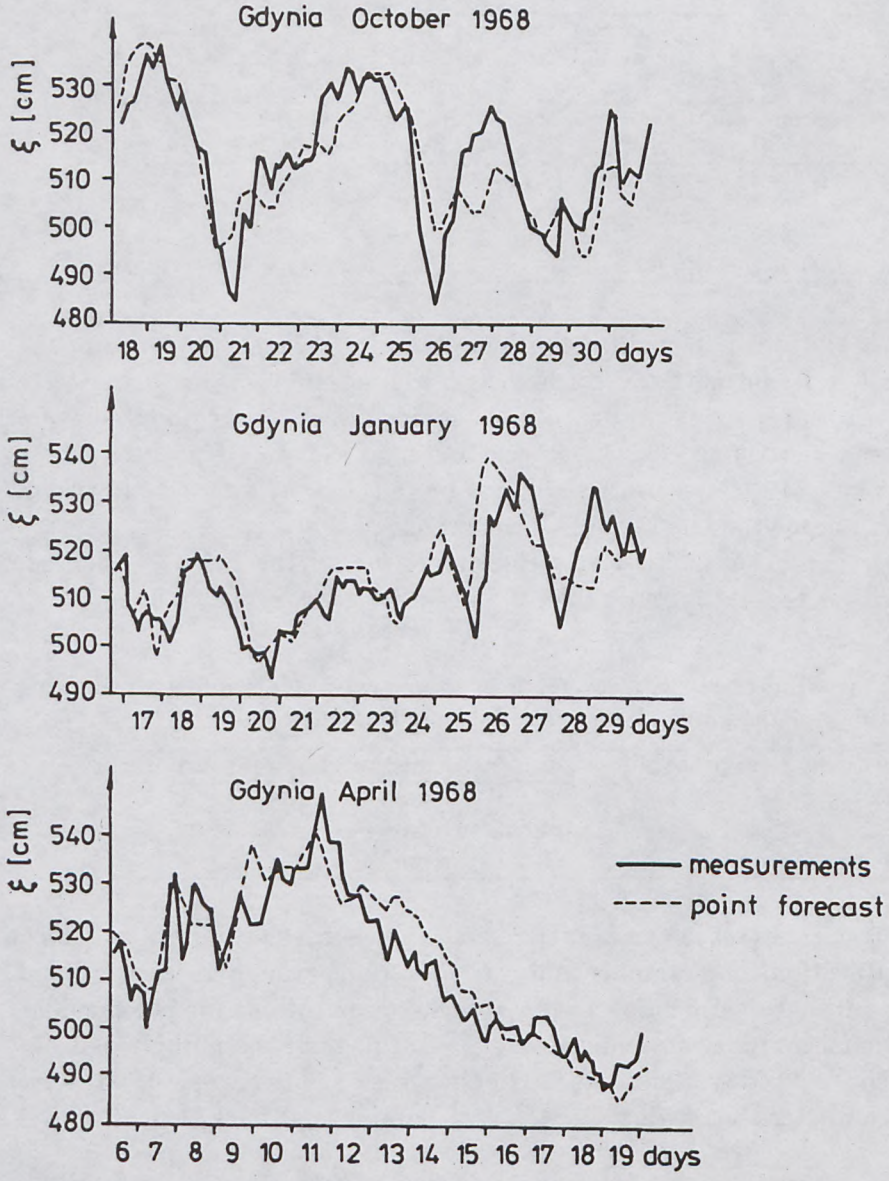

Fig. 6. Examples of sea level computations for independent observational material

Table 6. Verification of the model for independent observational material. Persistent forecast errors are given in brackets

Characteristics	Świnoujście [cm]	Kołobrzeg [cm]	Ustka [cm]	Władysławowo [cm]	Gdynia [cm]
σ_v					
for the period	9.4	10.2	8.9	8.5	7.9
01.10.1968 – 31.10.1968	[22.8]	[22.1]	[18.4]	[16.4]	[15.1]
σ_v					
for the period	10.6	9.9	7.8	7.3	7.9
01.01.1968 – 30.05.1968	[20.5]	[18.1]	[14.8]	[12.5]	[13.2]

changes. This enables the model to be tested under unfavourable conditions of atmospheric forcing. The computation results are given in Table 6. It can be inferred from this data that operation of the model under the assumed wind field conditions does not differ significantly from the results computed for long periods of the dependent material given in Table 3. The computation results for independent material under selected conditions of sea level changes are shown in Figure 6. As to the occurrence of forecast errors it should be emphasized that after long practical use the problem can be once more analyzed taking into account the error component resulting from the error in the atmospheric pressure field forecast. According to the experiments carried out in Sweden with models employing the EOF cited at the beginning of the paper, this component does not significantly change the magnitude of the mean errors obtained in the hindcast computations for a long period of time. These errors may, however, be decisive in the accuracy of storm surge forecasts.

6. Storm surge computations

The method considered is related to the computation errors which are characterized with reference to the real occurrence of the phenomenon. Such errors are inevitable in every forecast model, and the way to avoid these disadvantages is to introduce an interval forecast. This problem was dealt with in the literature by Kaczmarek (1969). The predictand in the interval forecast is not determined as a point value but its occurrence is related to a certain interval depending on the probability assumed. This assumption can be given by

$$P_\alpha = P(y_l \leq \hat{y} \leq y_u) = \int_{y_l}^{y_u} f(y|x_1, ..., x_k)dy, \tag{10}$$

where

P_α – the assumed probability,

l, u – lower and upper limit indices of predictand occurrence at a given probability,

$f(y|x_1, x_2, ..., x_k)$ – density of conditional probability distribution,

$\hat{y}$ – point forecast.

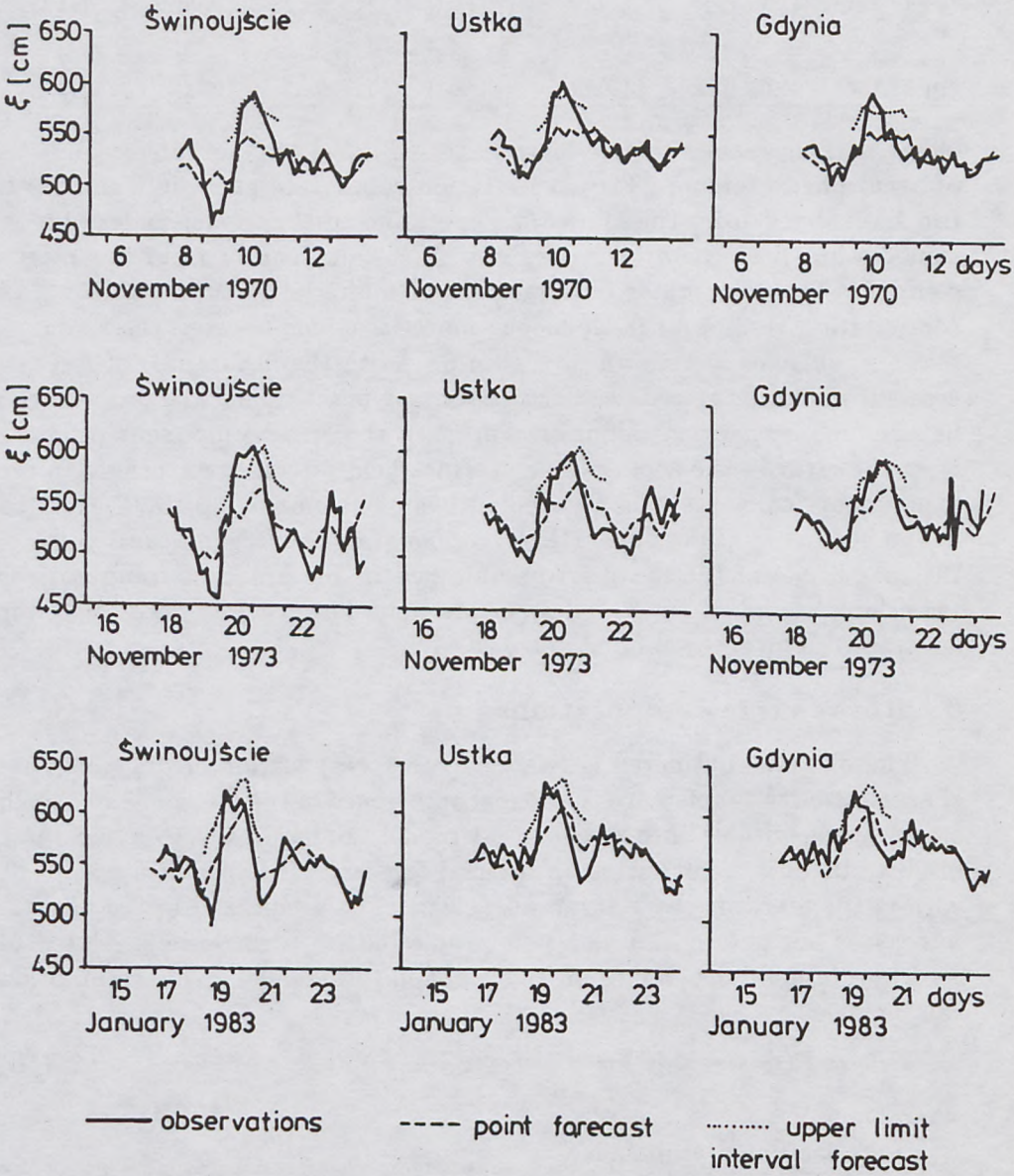

Fig. 7. Examples of storm surge computations for independent observational material

In the practical approach to the empirical probability, the illustrative computation results of formula (10) are given in Table 4. In everyday use, however, a problem emerges in introducing the upper or lower limit only instead of the whole predictand interval. In the case of the Polish coast this problem becomes simpler since rapid changes in the sea level result from very strong onshore (raising sea level) or offshore (falling sea level) winds. When forecasting such winds, depending on the assignment of the sea level forecast, a definite limit of the predictand interval can be used. The probability assumed for the sea level forecast should be related to the wind force and direction forecast, thus also embracing the analysis of the meteorological forecast effectiveness. The problem can be solved definitively after long use of the model in practice.

Table 7. Mean errors of the upper limit interval forecast model in hindcast computations of the seven greatest storm surges in 1970–1983

Świnoujście $< \|v\| >$ [cm]	Kołobrzeg $< \|v\| >$ [cm]	Ustka $< \|v\| >$ [cm]	Władysławowo $< \|v\| >$ [cm]	Gdynia $< \|v\| >$ [cm]
17	18	14	14	14

As can be initially inferred from Table 4, under the everyday conditions of wind vector occurrence, a point forecast can be applied. For a fresh onshore gale, the employment of the upper interval limit in five ports with a probability of 99.3% – 99.8% yields results enabling a sea level forecast satisfactory for shore protection to be formulated. If the forecast concerns the depth of fairways, the same probability degree can be used for strong and violent offshore winds. In the alternative approach, it is necessary to work out a separate forecast model for storm surges only. The interval forecast described has been checked for great storm surges. The results are presented in Table 7 and Figure 7.

7. Conclusion

The forecast presented is one more method which resolves into the application of EOF and the equations of multiple regression of dynamic systems. Even though essential modifications have been introduced in the representation of the sea level and atmospheric pressure field, the computations have once again demonstrated that the assumptions regarding the employment of EOF and the dynamic regression equations represent general physical relationships between the analyzed phenomena, thus constituting a basis for different statistical models.

The results confirm the usefulness of sampling the phenomena analyzed with a time interval of 3 h, and of the assumption that the sea level and the atmospheric pressure field changes are superimpositions of long- and short-period oscillations. These assumptions, together with the method employing the interval forecast, enable rapid sea level changes to be forecasted with a lead time of 24 h.

The analysis of the forecast errors revealed their statistical characteristics and confirmed the good operation of the model under various conditions of a changing atmospheric pressure field.

References

Golub G. H., Heath M., 1979, *Generalized cross-validation as a method for choosing a good Ridge parameter*, Technometrix, 21, 215–223.

Holmström I., Stokes J., 1978, *Statistical forecasting of sea level changes in the Baltic*, Swedish Meteorological and Hydrological Institute. Report RMK 9, 20 pp.

Institute of Meteorology and Water Management, Maritime Branch, 1983, Measurement Data, Gdynia,(unpublished).

Kaczmarek Z., 1969, *Errors in forecast models*, Wiad. Sł. Meteor. Hydr., 6(18), 11–25, (in Polish).

Kowalik Z., Wróblewski A., 1973, *Periodic oscillations of the sea level along the Polish coast of the Baltic*, Arch. Hydrotechn., 20, 203–213, (in Polish).

Lachenbruch P. A., Goldstein M., 1979, *Discriminant analysis*, Biometrics, 35, 69–85.

Nielsen P. B., 1979, *On empirical orthogonal functions EOF and their use for analysis of the Baltic Sea level*, Københavns Univ., Inst. Fys. Oceanogr., rep., 40, 37 pp.

Nyberg L., 1983, *Sea level forecast with an EOF model*, Proc. Intern. Symp. North Sea Dynamics, Springer–Verlag, 185–199.

Otnes R. K., Enochson I., 1972, *Digital time series analysis*, John Wiley and Sons, 388 pp., (in Polish).

Preisendorfer R. W., Barnett T. P., 1977, *Significance tests for empirical orthogonal functions*, Reprints 5-th Conf. Probability and Statistics, Las Vegas, Am. Meteor. Soc., 169–172.

Thompson K. R., 1979, *Regression models for monthly sea level*, Mar. Geodesy, 2, 269–290.

Törnevik H., 1977, *Application of empirical orthogonal functions to sea level forecasting*, ECMWF Workshop Empirical Orthogonal Functions in Meteor., 112–133.

Wróblewski A., 1986, *Application of EOF to computation of the storm surges on the Polish Baltic Coast in January 1983*, Acta Geophys. Pol., 34, 63–75.

Wróblewski A., 1990, *Statistical forecasting of random dynamic processes in the near-shore zone of the Southern Baltic*, Ossolineum, Wrocław, 126 pp., (in Polish).